ELSEVIER

Spectrochimica Acta Part A 51 (1995) L7–L21

SPECTROCHIMICA ACTA
PART A

Absorption and fluorescence properties of fluorescein

Robert Sjöback [1], Jan Nygren [1], Mikael Kubista *

Molecular Biotechnology Group, Department of Biochemistry and Biophysics, Chalmers University of Technology, S-413 90 Gothenburg, Sweden

Received 23 January 1995; accepted 7 February 1995

Abstract

We have characterized the protolytic equilibria of fluorescein and determined the spectroscopic properties of its protolytic forms. The protolytic constants relating the chemical activities (which at low ionic strength equal concentrations) of the cation, neutral form, anion and dianion are $pK_1 = 2.08$, $pK_2 = 4.31$, and $pK_3 = 6.43$. All forms have rather high molar absorptivities being $\varepsilon_{437}^{FH_2^+} = 53\,000$, $\varepsilon_{434}^{FH_2} = 11\,000$, $\varepsilon_{453}^{FH^-} = 29\,000$ ($\varepsilon_{472}^{FH^-} = 29\,000$) and $\varepsilon_{490}^{F^{2-}} = 76\,900\ M^{-1}\ cm^{-1}$ for the cation, neutral form, anion and dianion, respectively. The dianion has the most intense fluorescence with a quantum yield of 0.93 but also the anion shows considerable fluorescence with a quantum yield of 0.37. The neutral and cationic species are upon excitation converted into the anion and fluoresce with quantum yields of about 0.30 and 0.18, respectively.

1. Introduction

The fluorescein dye is probably the most common fluorescent probe today. Its very high molar absorptivity at the wavelength of the argon laser (488 nm), large fluorescence quantum yield and high photostability makes it a very useful and sensitive fluorescent label. Fluorescein is commercially available in many derivatives, such as fluorescein isothiocyanate and fluorescein succinimidyl ester, that can be covalently attached to macromolecules and to amino acids. The labeled molecules can be detected with very high sensitivity which is utilized in, for example, capillary electrophoresis [1,2]. The emission spectrum of fluorescein overlaps extensively the absorption spectrum of tetramethyl rhodamine, which is a related strongly fluorescent dye, making this pair very suitable for energy transfer experiments to determine distances within and between labeled macromolecules [3].

Fluorescein in aqueous solution occurs in cationic, neutral, anionic and dianionic forms [4] making its absorption and fluoresence properties strongly pH dependent. The protolytic constants relating the concentrations of the protolytic forms have been difficult to determine, because their spectra overlap substantially and the different pK_a values are quite close. Previous determinations have been based on rather crude assumptions about the spectral overlaps between the protolytic forms and have yielded rather scattered estimations of the protolytic constants [4,5]. With the recent advent of powerful chemometric methods for spectral analysis, complicated spectroscopic mixtures can today be

* Corresponding author.

[1] These authors have contributed equally to this work.

SSDI 0584-8539(95)01421-7

analyzed with confidence [6]. In this work we use these methods to determine the protolytic constants of fluorescein and to characterize the absorption, fluorescence excitation and fluorescence emission spectra of its protolytic forms.

2. Materials and methods

2.1. Chemicals

Fluorescein was purchased from Sigma and was used without further purification. Spectral analysis revealed that the dye did not contain any significant amounts of contaminants. Its concentration was determined spectroscopically assuming a molar absorptivity of 76 900 ($\pm$600) $M^{-1}\,cm^{-1}$ for the fluorescein dianion in 0.1 M NaOH, which was determined using carefully dried samples. This value is in good agreement with previous determinations [7–9]. Buffers used were phosphate at pH $\geqslant$ 5 and citrate at lower pH.

2.2. Spectroscopic measurements

Absorption spectra were measured on a CARY 2300 spectrometer, and fluorescence spectra on a SPEX Model FL1T1 τ2 spectrofluorometer. The optical path was 1 cm and spectra were collected at a resolution of five data points per nanometer. When recording fluorescence spectra the total absorption in no case exceeded 0.06, making the necessary correction for the inner filter effect small [10]. Fluorescence lifetime measurements were performed using a modulation technique on the SPEX fluorometer.

2.3. Determination of thermodynamic protolytic constants

The thermodynamic protolytic constant for an acid–base equilibrium

$$AH^n \overset{K_a}{\rightleftharpoons} A^{(n+1)} + H^+ \tag{1}$$

is given by

$$\frac{\{A^{(n+1)-}\}\{H^+\}}{\{AH^{n-}\}} = K_a \tag{2}$$

where the curved brackets indicate chemical activities and $K_a = 10^{-pK_a}$. Proton activity is measured through pH ($\{H^+\} = -\log\{H^+\}$) and component concentrations are determined by absorption measurements. These are related to chemical activities as $\{X\} = \gamma_X[X]$, where [X] is the concentration of species X and γ_X is its activity factor.

We define an apparent protolytic constant K'_a as the thermodynamic protolytic constant times the ratio of the activity factors of the protolytic species

$$K'_a = \frac{[A^{(n+1)-}]\{H^+\}}{[AH^{n-}]} = K_a\left(\frac{\gamma_{AH^{n-}}}{\gamma_{A^{(n+1)-}}}\right) \tag{3}$$

The activity factors depend on the ionic strength and can be estimated by the extended Debye–Hückel equation [11,12]

$$-\log\gamma_X \approx z_X^2 A I^{0.5}/(1 - BI^{0.5}) + C_X I \tag{4}$$

where z_X is the charge of X, A is a constant depending on solvent and temperature ($=0.509\ M^{-0.5}$ in aqueous solution at 25 °C) [13], $I = \frac{1}{2}\sum_i z_i^2 c_i$ is the ionic strength, and B is a constant that according to theory depends on the distance of closest approach between interacting ions, but is generally treated as an adjustable parameter. C_X is an empirical parameter not accounted for by theory, but required to account for the dependence at high ionic strength [14].

Eqs. (3) and (4) are combined to give

$$pK'_a = pK_a - (2n+1)AI^{0.5}/(1+BI^{0.5}) - CI \quad (5)$$

and fitted to the dependence of the apparent protolytic constants on ionic strength. The thermodynamic protolytic constant pK_a is obtained by extrapolation to zero ionic strength.

Samples were prepared from three stock solutions with identical concentrations of fluorescein in 5 mM buffer and also containing 0, 40 mM and 1 M NaCl, respectively. Measurements were made at a pH close to the pK'_a in 200 mM NaCl, which produces the largest changes in the relative concentrations of the protolytic forms and thus highest accuracy in the analysis.

Molar ratios $x_{A^{(n+1)-}}$ and $x_{AH^{n-}}$, of the protolytic forms were determined by decomposing the sample absorption spectra $S(\lambda)$ into a sum of their normalized spectral responses $A^{(n+1)-}(\lambda)$ and $AH^{n-}(\lambda)$

$$S(\lambda) = x_{A^{(n+1)-}} A^{(n+1)-}(\lambda) + x_{AH^{n-}} AH^{n-}(\lambda) \quad (6)$$

The sum of the molar ratios never deviated from unity by more than 2%, indicating successful analysis.

2.4. Determination of absorption spectra and apparent protolytic constants

Protolytic constants and absorption spectra of the protolytic forms were determined from absorption spectra recorded at various pH values. The procedure to analyze such titration data has been described in detail elsewhere [15], and is only briefly outlined here. The recorded absorption spectra are collected as rows in a matrix $\boldsymbol{A}$ which is decomposed using Nipals into a product of a target matrix $\boldsymbol{T}$, and a score matrix $\boldsymbol{P}'$, plus a residual $\boldsymbol{E}$

$$\boldsymbol{A} = \boldsymbol{T}\boldsymbol{P}' + \boldsymbol{E} \quad (7)$$

The concentrations of the protolytic forms are then calculated from the equilibrium expressions

$$\frac{[FH_2]\{H^+\}}{[FH_3^+]} = K'_1 \quad (8)$$

$$\frac{[FH^-]\{H^+\}}{[FH_2]} = K'_2 \quad (9)$$

$$\frac{[F^{2-}]\{H^+\}}{[FH^-]} = K'_3 \quad (10)$$

for various trial values of the apparent equilibrium constants and fitted to the columns of the target matrix

$$\boldsymbol{t}_i = \sum_{j=1}^{n} r_{ij}\hat{\boldsymbol{c}}_i \qquad (i,j = l,n) \quad (11)$$

where $\boldsymbol{t}_i$ is the ith column of matrix $\boldsymbol{T}$, $\hat{\boldsymbol{c}}_i$ is a vector containing the calculated concentration of protolytic form i from Eqs. (8)–(10), and n is the number of protolytic forms considered. r_{ij} are elements of a matrix $\boldsymbol{R}$ which rotates the target and projection matrices to give new concentrations $\boldsymbol{C}$, and spectral profiles $\boldsymbol{V}$, of the protolytic forms

$$\boldsymbol{C} = \boldsymbol{T}\boldsymbol{R}^{-1} \quad (12)$$

$$\boldsymbol{V} = \boldsymbol{R}\boldsymbol{P}' \quad (13)$$

The trial values of the protolytic constants are systematically varied to give highest correspondence between the concentrations calculated from the equilibrium Eqs. (8)–(10) and those calculated by Eq. (12). Absorption spectra are calculated from Eq. (13) and

normalized by the molar absorptivity of the fluorescein dianion at 490 nm (76 900 M^{-1} cm^{-1}).

2.5. Determination of fluorescence excitation and emission profiles

The fluorescence intensity of a sample mixture observed at emission wavelength λ_{em}, upon illumination at excitation wavelength λ_{ex}, is

$$I(\lambda_{ex}, \lambda_{em}) = \kappa \sum_{i=1}^{n} c_i \varepsilon_i(\lambda_{ex}) \Phi_i(\lambda_{ex}) I_i(\lambda_{em}) = \kappa \sum_{i=1}^{n} c_i I_i(\lambda_{ex}) I_i(\lambda_{em}) \quad (14)$$

where κ is an instrument parameter and n is the number of fluorescent components. c_i, $\varepsilon_i(\lambda_{ex})$, $\Phi_i(\lambda_{ex})$ and $I_i(\lambda_{em})$ are the concentration, molar absorptivity, fluorescence quantum yield and normalized emission of the ith component, and $I_i(\lambda_{ex}) = \Phi_i(\lambda_{ex})\varepsilon_i(\lambda_{ex})$ is its fluorescence excitation spectrum. Note that for each individual component $I(\lambda_{em})$ and $I(\lambda_{ex})$ are independent of λ_{ex} and λ_{em}, respectively.

Emission spectra of the fluorescein protolytic forms were determined from emission spectra recorded at different excitation wavelengths of two samples of somewhat different pH. These spectra are described by the equations

$$I(\lambda_{em})^{pH_1}_{\lambda_{ex}} = \kappa \sum_{i=1}^{n} I_i(\lambda_{ex}) c_i^{pH_1} I_i(\lambda_{em}) \quad (15)$$

$$I(\lambda_{em})^{pH_2}_{\lambda_{ex}} = \kappa \sum_{i=1}^{n} I_i(\lambda_{ex}) c_i^{pH_2} I_i(\lambda_{em}) \quad (16)$$

which can be written in matrix form

$$\boldsymbol{A} = \boldsymbol{CV}$$

$$\boldsymbol{B} = \boldsymbol{CDV} \quad (17)$$

Here matrices $\boldsymbol{A}$ and $\boldsymbol{B}$ contain the recorded emission spectra as rows, matrix $\boldsymbol{C}$ contains fluorescence excitation intensities of the components, $I_i(\lambda_{ex})$ as columns, matrix $\boldsymbol{V}$ their emission spectra $I_i(\lambda_{em})$ as rows, and $\boldsymbol{D}$ is a diagonal matrix containing their concentration ratios $c_i^{pH_2}/c_i^{pH_1}$. Equation system (17) was solved for $\boldsymbol{C}$, $\boldsymbol{D}$, and $\boldsymbol{V}$ by the Procrustes rotation method using the DATa ANalysis program (DATAN) [16,17]. Excitation spectra of the protolytic forms were determined analogously from excitation spectra of the two samples recorded at different emission wavelengths.

2.6. Determination of fluorescence quantum yields

Fluorescence quantum yields were determined by different approaches depending on whether protolytic reactions take place in the excited state or not. This is readily recognized from experimental data, because if protolytic equilibrium is attained in the excited state the shape of the emission spectrum is independent of excitation wavelength (and the shape of the excitation spectrum is independent of emission wavelength), whereas if excited state reactions do not take place the protolytic forms behave as independent species and the shape of the emission spectrum changes with excitation wavelength (and excitation spectrum with emission wavelength).

2.6.1. Independent species

Emission spectra $I(\lambda_{em})_{\lambda_{ex}}$, recorded on a sample containing two independent species are weighted sums of their contributions $I_i(\lambda_{em})$

$$I(\lambda_{em})_{\lambda_{ex}} = k_1(\lambda_{ex}) I_1(\lambda_{em}) + k_2(\lambda_{ex}) I_2(\lambda_{em}) \quad (18)$$

The weights depend on the excitation wavelength used (see Eq. (14))

$$k_i(\lambda_{ex}) = c_i \varepsilon_i(\lambda_{ex}) \Phi_i(\lambda_{ex}) \kappa \quad (19)$$

and are determined by decomposing the emission spectra into the known profiles of the components. The weights are then combined to give the ratio between the fluorescent quantum yields of the two species

$$\frac{\Phi_1(\lambda_{ex})}{\Phi_2(\lambda_{ex})} = \frac{k_1(\lambda_{ex})c_2\varepsilon_2(\lambda_{ex})}{k_2(\lambda_{ex})c_1\varepsilon_1(\lambda_{ex})} \tag{20}$$

Absolute values of the fluorescence quantum yields are obtained by assuming a wavelength independent quantum yield of 0.93 for the fluorescein dianion [18–20].

2.6.2. Interconverting species

If upon excitation one protolytic species is converted into another species, the quantum yield for the conversion $\Phi^e_{1\to 2}$ can be determined from the dependence of emission intensity on pH

$$I(\mathrm{pH}_i)_{\lambda_{ex}} = \kappa(c_1(\mathrm{pH}_i)\varepsilon_1(\lambda_{ex})\Phi^e_{1\to 2} + c_2(\mathrm{pH}_i)\varepsilon_2(\lambda_{ex}))\Phi^f_2(\lambda_{ex}) \tag{21}$$

where $\Phi^f_2(\lambda_{ex})$ is the fluorescence quantum yield of the emitting species. The quantum yields $\Phi^e_{1\to 2}$ and Φ^f_2 are determined by fitting the intensity dependence to the concentration profiles of the components. The approach does not require the quantum yields to be independent of excitation wavelength, but requires them to be independent of pH. This is in general the case for the fluorescence quantum yield, but not for the yield of conversion. Because the two species are protomers their equilibrium concentrations will depend on pH; further, the rate of conversion is often catalyzed by the appropriate protolytic form of the buffer, whose concentration depends on pH. Thus for the approach to be applicable data must be collected in a pH range significantly far from the pK^*_a of the excited state protolytic equilibrium, and the mechanism must be independent of buffer ions. As we shall see, these conditions are fulfilled for the fluorescein system.

For a more complex situation involving a third species that is converted to the luminescent form by two successive protonation reactions, the intensity depends on pH as

$$I(\mathrm{pH}_i)_{\lambda_{ex}} = \kappa[c_1(\mathrm{pH}_i)\varepsilon_1(\lambda_{ex})\Phi^e_{1\to 2}\Phi^e_{2\to 3} + c_2(\mathrm{pH}_i)\varepsilon_2(\lambda_{ex})\Phi^e_{2\to 3} + c_3(\mathrm{pH}_i)\varepsilon_3(\lambda_{ex})]\Phi^f_3(\lambda_{ex}) \tag{22}$$

where $\Phi^e_{1\to 2}$ and $\Phi^e_{2\to 3}$ are the yields of converting species 1 to species 2 and species 2 to species 3, respectively, in the excited state.

3. Results

3.1. Absorption titration

Fig. 1 left shows absorption spectra of fluorescein recorded in the pH range 2–10 in 50 mM buffer. Analysis of the titration data revealed the presence of four protolytic forms, which have previously been identified as the cation, neutral species, anion and dianion [15], and produced the spectra and concentrations shown in the middle and bottom panels. A corresponding titration in the presence of 1 M NaCl is shown to the right in the same figure. The calculated spectra of the protolytic forms from the two titrations are more or less identical, indicating successful analysis. The dianion has its main absorption peak at 490 nm (76 900 $M^{-1}\,cm^{-1}$), with a shoulder around 475 nm. It has very weak absorption in the region 350–440 nm, and distinct absorption peaks in the UV region at 322 (9500 $M^{-1}\,cm^{-1}$), 283 (14 400 $M^{-1}\,cm^{-1}$) and 239 (43 000 $M^{-1}\,cm^{-1}$) nm. The anion has somewhat weaker absorption in the visible region with peaks at 472 and 453 nm of roughly the same molar absorptivity (29 000 $M^{-1}\,cm^{-1}$). It absorbs weakly in the near UV region, and has peaks at 310 (7000 $M^{-1}\,cm^{-1}$) and 273 (17 000 $M^{-1}\,cm^{-1}$) nm. The neutral species has by far lowest absorption in the visible region, with a maximum at 434 nm (11 000 $M^{-1}\,cm^{-1}$) and a side maximum at 475 nm (3600 $M^{-1}\,cm^{-1}$). Its absorption below 400 nm is very small.

The cation has maximum absorption at 437 nm (53 000 M^{-1} cm^{-1}), and two additional peaks at 297 (7100 M^{-1} cm^{-1}) and 250 (33 000 M^{-1} cm^{-1}) nm.

In contrast to the absorption spectra the calculated concentration dependencies on pH of the protolytic forms are different in the two titration sets. The apparent protolytic constants are $pK'_1 = 2.09$, $pK'_2 = 4.30$, and $pK'_3 = 6.41$ in pure buffer, and $pK'_1 = 2.14$, $pK'_2 = 4.20$, and $pK'_3 = 6.00$ in the presence of 1 M NaCl. This difference, which is due to the dependence of the activity factors on ionic strength (Eqs. (3)–(6)), was studied more extensively for the equilibrium between the anion and dianion. Fig. 2 shows absorption spectra at pH 6.14 recorded at various salt concentrations in the range 0–1 M NaCl. Only 5 mM buffer was used to adjust the pH, so essentially all ionic strength is due to the salt. At this pH only and anion and dianion are present, as evidenced by the distinct isosbestic point at 462 nm. With increasing ionic strength the intensity of the 490 nm peak grows due to accumulation of the dianionic species, as expected owing to its higher charge. Molar ratios of the two forms in the samples were determined by decomposing the spectra into their contributions (Eq. (6)), and apparent protolytic constants pK'_3 were calculated (Eq. (10)). These are plotted versus the square-root of the ionic strength in Fig. 3, which also includes data from a similar titration made at pH 6.09. The data from the two titrations are in excellent congruence, as expected, because pH should not affect the ionic strength dependence. The data were fitted by Eq. (5), which gave a thermodynamic protolytic constant pK_3 of 6.43 (and $B = 2.96$ $M^{-0.5}$ and $C = 0.135$ M^{-1}).

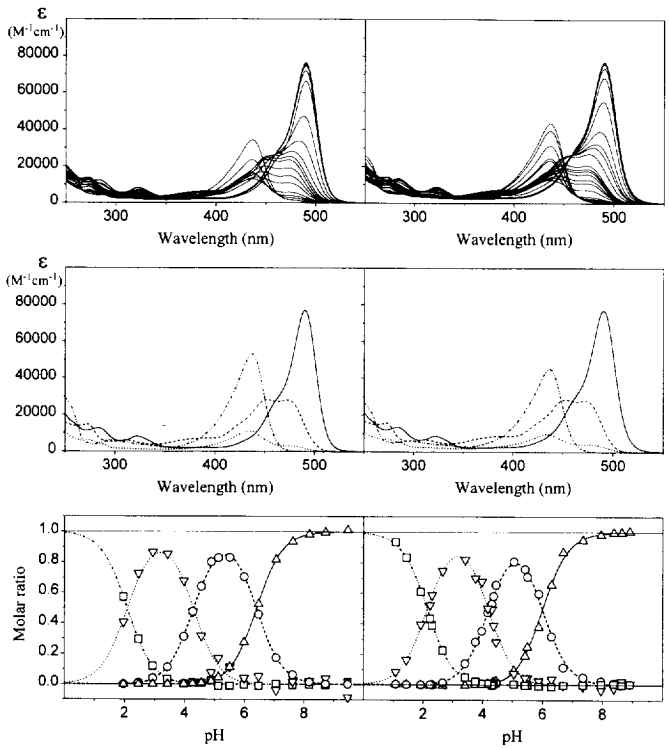

Fig. 1. Top: Absorption spectra of fluorescein (14 μM) in 50 mM buffer (expressed in molar absorptivities assuming $\varepsilon_{490} = 76\,900$ M^{-1} cm^{-1} for the dianion). Left: In absence of salt. Spectra recorded at pH 1.97, 2.47, 2.94, 3.43, 3.98, 4.27, 4.56, 4.89, 5.13, 5.51, 5.99, 6.47, 7.06, 7.62, 8.18, 8.72, 9.47. Right: In presence of 1 M NaCl. Spectra recorded at pH 1.08, 1.44, 1.92, 2.24, 2.30, 2.66, 3.41, 3.76, 3.97, 4.17, 4.31, 4.37, 4.45, 5.05, 5.42, 5.50, 5.88, 6.30, 6.69, 7.35, 7.95, 8.38, 8.64, 8.99. Middle: Calculated spectral responses of the four protolytic forms (cation, – · · –; neutral species, · · · ·; anion, – – –; dianion, ——). Bottom: Calculated concentrations of the cation (□), neutral species (▽), anion (○), and dianion (△) compared to concentrations predicted by the calculated protolytic constants (line coding as above).

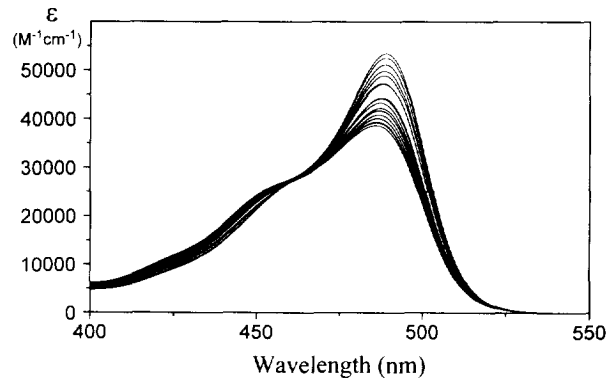

Fig. 2. Absorption spectra of fluorescein (20 μM) in 5 mM buffer adjusted to pH 6.14 in the presence and 0, 0.4, 1.6, 3.6, 6.4, 10.0, 14.4, 19.6, 25.6, 32.4, 40.0, 62.5, 90.0, 160, 250, 360, 490, 640, 810 and 1000 mM NaCl. Intensity at 490 nm increases with increasing ionic strength.

3.2. Temperature dependence

Both spectral responses and protolytic constants were found to depend on temperature. In the range 4–80°C the low energy absorption band of both the anion and dianion shifts to higher wavelength by about 0.07 nm $°C^{-1}$, and the protolytic constant decreases by about 0.008 units $°C^{-1}$ (results not shown). Analysis of the data by means of a van't Hoff plot gave a molar enthalpy change of about 9.8 kJ mol^{-1}. The temperature dependence of the other protolytic constants was not studied.

3.3. Fluorescence spectra at neutral and weakly acidic pH

Fluorescence excitation spectra recorded at different emission wavelengths and emission spectra recorded at different excitation wavelengths, of samples with pH 5.56 and 6.53, are shown in Figs. 4 and 5. In each set the spectral shapes vary considerably demonstrating the presence of at least two independent fluorescent species. This was confirmed by Procrustes rotation analysis, which revealed the presence of two fluorescent components. Because neutral, anionic and dianionic protolytic forms are present in this pH range (see Fig. 1), we conclude that only two of these fluoresce.

Calculated excitation and emission profiles of the two components are shown in the bottom panels. These can be identified from the calculated concentration ratios $c_i^{pH_2(=6.53)}/c_i^{pH_1(=5.56)}$, obtained as elements of the $\boldsymbol{D}$ matrix (Eq. (17)). Analysis of

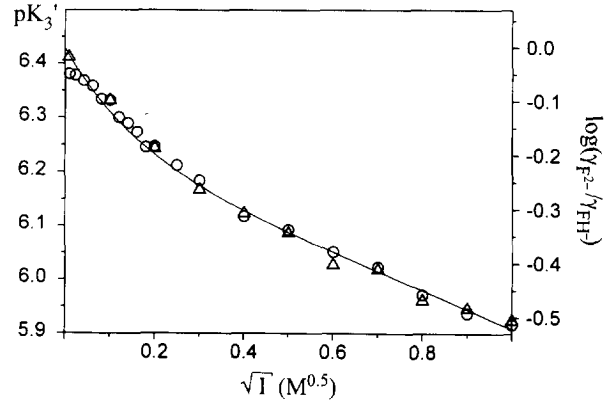

Fig. 3. Apparent protolytic constants (left scale) determined from the absorption spectra in Fig. 2 (○), and in a similar titration performed at pH 6.09 (△), plotted versus the square root of ionic strength. The data are fitted by Eq. (5). Right scale refers to the logarithm of the ratio between the activity factors of the dianion and anion. See text for details.

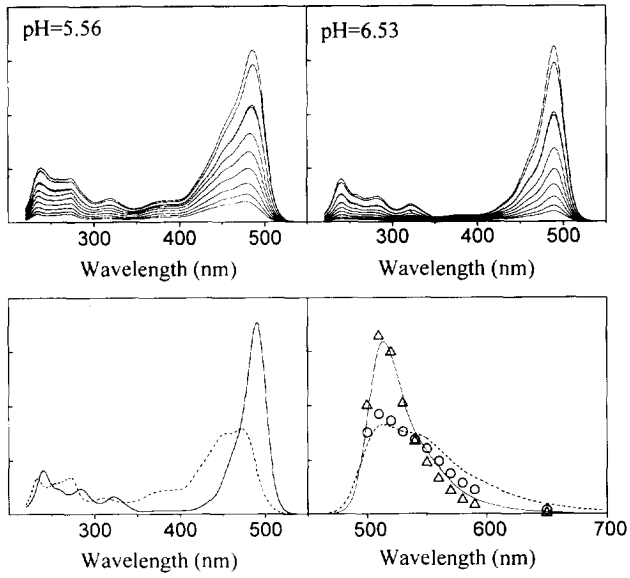

Fig. 4. Top: Fluorescence excitation spectra of fluorescein (0.20 μM) in 5 mM phosphate buffer at pH 5.56 (left) and pH 6.53 (right) using 500, 510, 520, 530, 540, 550, 560, 570, 580, 590 and 650 nm emission. Bottom: Left: Calculated excitation spectra of the anion (– – –) and dianion (——) scaled to the same areas. Right: Calculated emission intensities of the anion (○) and dianion (△). The lines are redrawn from the determination of emission spectra in Fig. 5.

excitation spectra gave the ratios 0.44 and 3.22, and analysis of emission spectra gave 0.48 and 4.47. The concentration ratios for the neutral species, anion and dianion calculated from the protolytic constants determined above are 0.05, 0.49 and 4.60, respectively. Clearly, the fluorescent species should be the anion and dianion, a conclusion also supported from the similarity of their absorption spectra and the calculated excitation spectra.

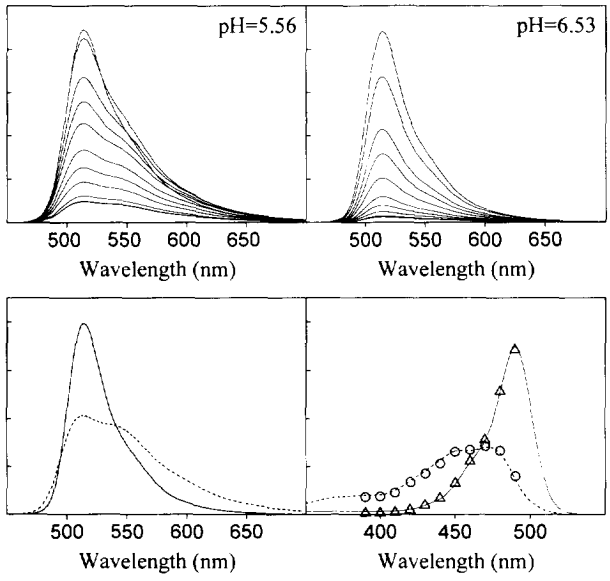

Fig. 5. Top: Fluorescence emission spectra of fluorescein (0.20 μM) in 5 mM phosphate buffer at pH 5.56 (left) and pH 6.53 (right) using 390, 400, 410, 420, 430, 440, 450, 460, 470, 480 and 490 nm excitation. Bottom: Left: Calculated emission spectra of the anion (– – –) and dianion (——) scaled to the same area. Right: Calculated excitation intensities of the anion (○) and dianion (△). The lines are redrawn from the determination of excitation spectra in Fig. 4.

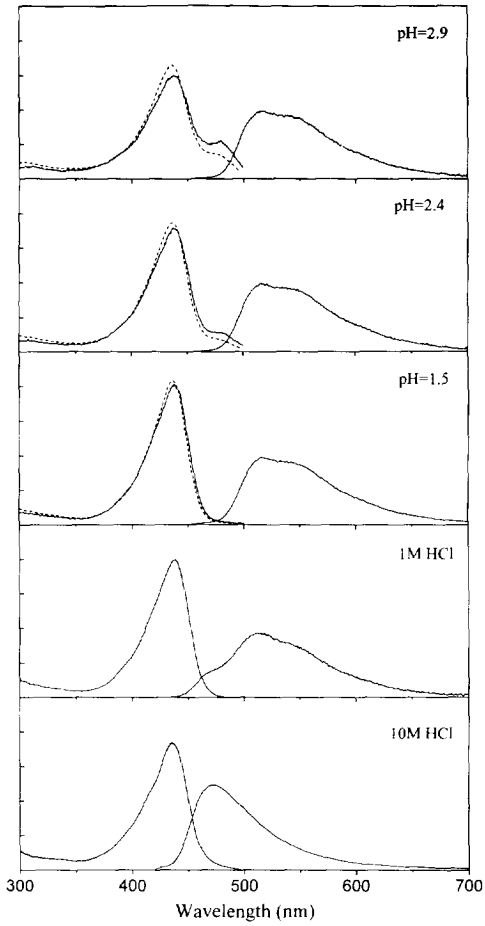

Fig. 6. Absorption spectra (– –), fluorescence excitation and emission spectra (——) of fluorescein in 50 mM buffer at pH 2.9, 2.4 and 1.5, and in 1 and 10 M HCl. For the last two samples absorption spectra were identical to the excitation spectra (not shown).

By decomposing the emission spectra into contributions from the anion and dianion the fluorescence quantum yield of the anion was determined (Eq. (20)). From the spectra recorded with 450, 460, 470 and 480 nm excitation an average value of the anion fluorescence quantum yield of 0.38 ± 0.02 was obtained.

3.4. Fluorescence at acidic pH

Fig. 6 shows absorption, and fluorescence excitation and emission spectra of fluorescein at low pH. At pH 2.9, 2.4, and 1.5 absorption and fluorescence excitation spectra display features of both the cation (the intense peak at 437 nm) and neutral species (shoulder at 4.75 nm), evidencing that both forms are present and give rise to fluorescence emission. The excitation/absorption ratio is larger at 475 nm than at 437 nm, implying more efficient fluorescence when the neutral species is excited. The shapes of the emission spectra are independent of excitation wavelength and the shapes of excitation spectra are independent of emission wavelength, meaning that the same species fluoresce independently of the protolytic form excited. Consequently protolytic equilibrium must be established in the excited state.

The shapes of the emission spectra are also independent of pH. By comparison with the spectra in Fig. 5 the emitting species can be identified as the fluorescein anion. Because essentially no anion is present in the ground state in this pH range, it must be formed by deprotonation of the cation and neutral species in the excited state. This in

turn implies that the second excited state protolytic constant pK_2^* is considerably lower than the corresponding ground state protolytic constant pK_2.

Even in 1 M HCl some anion fluorescence is observed, although additional emission is seen around 470 nm evidencing the presence of a different fluorescent species. In 10 M HCl all anion emission is lost and the novel emission predominates.

3.5. Dependence of fluorescence intensity on pH

Fig. 7 (top) shows fluorescence emission spectra recorded with 430 (left) and 450 (right) nm excitation at different pH in the interval 2–8. In this range all four protolytic forms are represented in ground state (see Fig. 1). Nipals treatment (Eq. (7)) of the entire data set revealed the presence of two emitting species, whereas successive analysis by Procrustes rotation (Eq. (17)) revealed that at least three (ground state) species give rise to the emission intensity, one giving rise to dianion and the others to anion emission (results not shown). In general Procrustes analysis of a data set such as that in Fig. 7 determines both the spectral profiles and concentrations of all components [17]. However, owing to the excited state reactions the experimental data are linear dependent and the concentrations determined by the analysis are unknown linear combinations of the true concentrations [16]. Therefore a somewhat different approach must be used.

We first analyzed the subset of spectra recorded in the pH range 5.4–8, where the anion and dianion are the only ground state protolytic forms present, and Procrustes analysis should work. The calculated spectra are in excellent agreement with those determined from the excitation/emission data in Fig. 5 and the calculated concentrations display a pH dependence characteristic of a protolytic equilibrium (Fig. 7, middle). Note

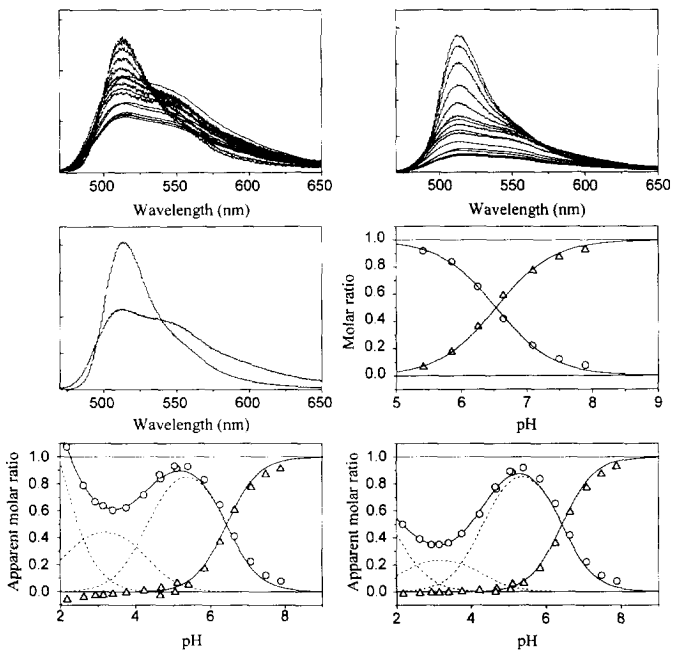

Fig. 7. Top: Fluorescence emission spectra of fluorescein (0.13 μM) in 5 mM buffer at pH 2.17, 2.62, 2.93, 3.14, 3.39, 3.75, 4.22, 4.65, 4.68, 5.05, 5.11, 5.41, 5.85, 6.25, 6.64, 7.09, 7.49 and 7.89, using 430 (left) and 450 (right) nm excitation. Middle: Results of Procrustes rotation analysis of the samples with $5.41 \leqslant pH \leqslant 7.89$. Left: Emission spectra of the anion (– – –) and dianion (——). Right: Molar ratios of the anion (○) and dianion (△). The solid line is the best fit assuming protolytic equilibrium ($pK_3' = 6.5$). Bottom: Contributions of anion (○) and dianion (△) emission to the total emission observed when using 430 (left) and 450 (right) nm excitation. Dashed lines are contributions to the total emission from the ground state species, determined by Eq. (22), solid lines are the sums of these contributions separated into anion and dianion emission.

Table 1
Summary of absorption, fluorescence and protolytic properties of fluorescein

	FH_3^+	FH_2	FH^-	F^{2-}
$\varepsilon/M^{-1}\,cm^{-1}$ (λ/nm)	53000(437)	3600(475)	29000(472)	76900(490)
$\varepsilon/M^{-1}\,cm^{-1}$ (λ/nm)	7100(297)	11000(434)	29000(453)	9500(322)
$\varepsilon/M^{-1}\,cm^{-1}$ (λ/nm)	33000(250)		700(310)	14000(283)
$\varepsilon/M^{-1}\,cm^{-1}$ (λ/nm)			17000(273)	43000(239)
τ/ns			3.0	4.1
Φ^f	~0(pH > 1.5)	~0	0.37	0.93
Φ^c	0.6	0.8	–	
pK'_a(1 M)	2.14	4.20	6.0	
pK'_a(50 mM)	2.09	4.30	6.41	
pK_a	2.08	4.31	6.43	

that Procrustes analysis does not force the calculated concentrations to obey an equilibrium relation, which was the case for the analysis of the absorption spectra. Fitting the calculated molar ratios to a protolytic equilibrium, we obtained pK_3^f 6.5 which is in fair agreement with pK_3 6.43 determined from the absorption data. From the areas of the calculated emission spectra, and the molar absorptivities of the anion and dianion at the two excitation wavelengths, the fluorescence quantum yield of the anion was calculated to be 0.37.

The complete set of emission spectra was then decomposed into contributions from anion and dianion emission (Fig. 7, bottom). While the dianion contribution is proportional to its ground state concentration, the anion contribution is not. It increases below pH 3.5 and, with 430 nm excitation at pH < 2.5, it becomes even larger than for pure anion! This is direct evidence that excitation of the cation and neutral species gives rise to anion emission. By fitting the anion contribution to the ground state concentration profiles of the three species (Eq. (22)), the yields of conversion were estimated to be 0.6 and 0.8 for $(FH_3^+)^* \rightarrow (FH_2)^*$ and $(FH_2)^* \rightarrow (FH^-)^*$, respectively.

3.6. *Fluorescence lifetimes*

For pure dianion in 0.1 M NaOH a single fluorescence lifetime of 4.1 ns was observed (Table 1). At pH 5.14, where both anion and dianion are present, fluorescence lifetimes of 4.1 and 3.0 ns were observed at all combinations of excitation and emission wavelengths. Because the longer lifetime is due to the dianion, the lifetime of the anion should be about 3 ns. At pH 3.17, where the dominant form is the neutral species, a single fluorescence lifetime of 3.1 ns was observed. Because the neutral species has no fluorescence of its own, this is the lifetime for the process of converting excited neutral species to anion followed by anion emission.

4. Discussion

The chemical structures of the fluorescein protolytic forms are shown in Fig. 8. The cation and dianion are expected to occur in only one chemical form. The neutral species can be obtained as a solid as a colorless lactone, yellow zwitterion or red *p*-quinoid [21]. In aqueous solutions the quinoid is generally believed to be prevalent [22]. Two chemical forms of the anionic species, with the negative charge either on the carboxylate group or on a ring hydroxyl, can be anticipated. Of these, the carboxylate form is expected to dominate owing to the generally more acidic character of this group. In addition to these monomeric forms, dimeric species have been reported [23]. However, under our conditions ($\leqslant$20 μM fluorescein, $\leqslant$1 M salt) dimerization was found to be negligible.

4.1. Ground state protolytic equilibria

Spectroscopic responses are proportional to component concentrations and not to chemical activities. As a consequence (apparent) equilibrium constants determined spectroscopically may deviate from the thermodynamic constants owing to sample non-ideality. As seen from the effect of ionic strength on the apparent protolytic constants for the anion/dianion equilibrium (Figs. 1 and 3) the difference may be substantial: in the range 0–1 M NaCl pK'_3 decreases by 0.41.

Rearranging Eq. (3) gives

$$pK'_a - pK_a = \log\left(\frac{\gamma_{A^{(n-1)-}}}{\gamma_{AH^{n-}}}\right) \tag{23}$$

and we see that the difference between the spectroscopically determined apparent protolytic constant pK'_a and the thermodynamic protolytic constant pK_a equals the logarithm of the ratio between the activity factors of the protolytic species involved in the equilibrium. Substracting 6.43 ($=pK_a$) from the apparent protolytic constants we obtain the logarithms of the ratios of the activity factors as a function of ionic strength (right scale in Fig. 3). Because protolytic forms always differ in charge, this has the interesting consequence that individual activity factors may be determined for the special case when the protolytic equilibrium involves an uncharged species. Activity factors for uncharged species deviate negligibly from unity (see Eq. (4)), and a good estimate of the activity factor of the charged species may be obtained. Because most techniques, such as electrochemical methods, only provide average activity factors of electrolyte species, this approach may be an interesting complement.

For the fluorescein system characterization of the ionic strength dependence on pK_2 is difficult, because conditions cannot be found where only the neutral and anionic species are present throughout the ionic strength interval, and pK_1 cannot be analyzed either, owing to the ionic strength contribution from the buffer required to maintain sufficiently low pH. However, knowing pK_3 and the dependence of pK'_3 on ionic strength, we can

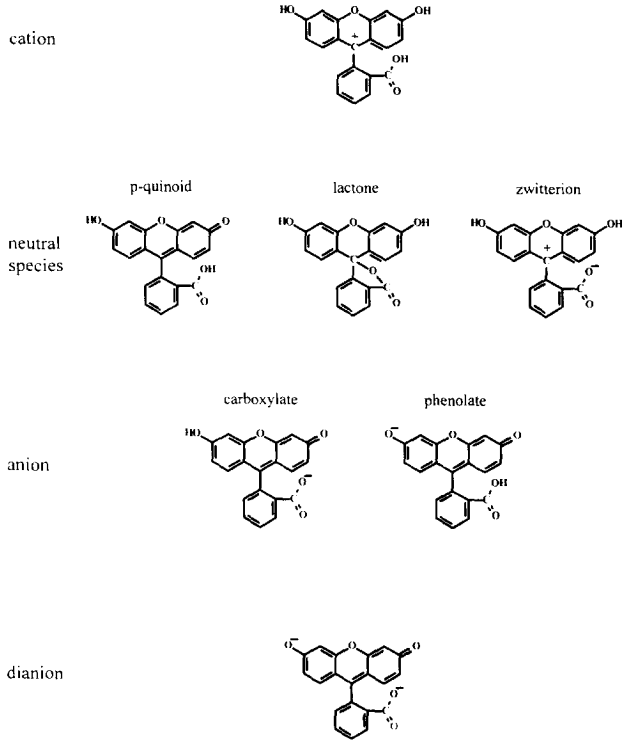

Fig. 8. Chemical structures of fluorescein.

estimate the other thermodynamic protolytic constants. The effect of salt is to stabilize charged species, thereby shifting protolytic equilibria towards the more highly charged protolytic form (Eq. (5)), thus increasing pK'_1 and decreasing pK'_2 and pK'_3 (Table 1). At low ionic strength CI in Eq. (5) is negligible and the difference $pK'_a - pK_a$ is proportional to the charge of the acidic protolytic species. Thus, with increasing ionic strength, pK'_2 should decrease and pK'_1 increase by about one third the magnitude of the change in pK'_3. In 50 mM buffer pK'_3 is 0.02 units lower than pK_3 (Table 1), yielding $pK_1 = pK'_1(50\ \text{mM}) - 0.02/3 \approx 2.08$ and $pK_2 = pK'_2(50\ \text{mM}) + 0.02/3 \approx 4.31$.

4.2. *Protolytic equilibria in excited state*

Protolytic constants of electronically excited molecules are often very different from those of the ground state owing to the substantially altered charge distribution in the excited species [24]. These protolytic constants may be determined from the effect of pH on fluorescence intensity if equilibrium is established in the excited state prior to de-excitation [24]. Such experiments have been performed with fluorescein and values of the excited state protolytic constants have been reported [25]. However, owing to the very short lifetimes of the fluorescein species (3–4 ns) it is questionable if protolytic equilibria are established in excited state. Let us make a rough estimate of the rates of the various faiths of excited fluorescein dianion. Its fluorescence lifetime τ is about 4 ns (Table 1), corresponding to a rate of de-excitation proportional to $\tau^{-1} = 2.5 \times 10^8\ \text{s}^{-1}$. Protolytic reactions are usually catalyzed by buffer ions and occur with a rate proportional to $k_b[\text{B}]$, where [B] is the concentration of the appropriate protolytic form of the buffer ions. For similar systems k_b has been experimentally determined to be about $1 \times 10^9\ \text{M}^{-1}\ \text{s}^{-1}$ [26]. Thus, for protolysis in the excited state to be as effective as spontaneous de-excitation of the fluorescein dianion, the concentration of the appropriate buffer species (in this case the acidic form) must be $[\text{BH}] \approx 2.5 \times 10^8/1 \times 10^9 = 0.25$ M. At a pH around pK_a of the buffer, this corresponds to a total buffer concentration of about 500 mM. For protolytic equilibrium to be fully established in the excited state, even higher buffer concentrations would be required. We therefore find it very unlikely that protolytic equilibria are fully established in the excited state by means of buffer catalysis for the fluorescein system.

4.2.1. *The anion–dianion protolytic equilibrium*

If propolytic equilibrium were attained in the excited state, the shape of emission spectrum should be independent of excitation wavelength and vice versa. This is clearly not the case for the anion–dianion equilibrium, where a substantial dependence is observed (Figs. 4 and 5). In fact, because the determined excitation spectra (Fig. 4) are very similar in shape to the corresponding absorption spectra (Fig. 1), and the protolytic constants determined by fluorescence (6.5) and by absorption (6.43) are close, it is more likely that protolysis in the excited state is insignificant. We therefore conclude that protolytic equilibrium between fluorescein anion and dianion is not attained in the excited state and that reported experimental determinations of pK_3^* are erroneous.

Although the excited state protolytic constant for the anion–dianion equilibrium cannot be determined, it may be estimated by the Förster cycle [24]. From the determined excitation and emission spectra (Figs. 4 and 5) we estimate the $S_0 \rightarrow S_1$ energy differences to be 20 169 and 19 951 cm^{-1} for the anion and dianion, respectively, which gives $pK_3^* = 6.43\ (+pK_3) - 0.46 = 5.97$.

4.2.2. *Fluorescence quantum yields of the anion and dianion*

The absorption (Fig. 1) and fluorescence excitation (Fig. 4) spectra of the fluorescein dianion are in perfect congruence above 300 nm, evidencing a wavelength-independent fluorescence quantum yield in this region. It has been determined previously by several authors to be about 0.93 [18–20], and was not considered necessary to verify. Below 300 nm the relative intensity of the fluorescence excitation spectrum decreases in comparison to the absorption spectrum by about 50% evidencing a corresponding decrease in the fluorescence quantum yield.

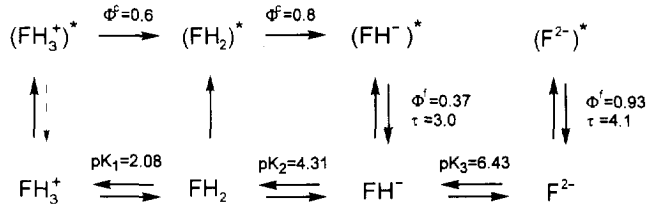

Scheme 1. Ground and excited state reactions of fluorescein.

The anion fluorescence quantum yield was determined by two approaches to be about 0.37 (Figs. 5 and 7). Comparison of its absorption (Fig. 1) and fluorescence excitation (Fig. 4) spectra reveals some differences in shapes: in absorption the maxima at 453 and 472 nm are of equal magnitudes, whereas in excitation the maximum at 472 nm is larger. This suggests the anion fluorescence quantum yield decreases somewhat with decreasing excitation wavelength. Because emission of most species originates from the lowest vibrational level of the first excited state [27], pure species in general have wavelength independent fluorescence quantum yields. This observation may therefore be an indication that two chemical forms of the anion are present (Fig. 8).

4.2.3. The cation and neutral species

At pH 1.5–3, where the cation and neutral species are the protolytic forms present in the ground state, anion emission is observed due to deprotonation in excited states (Fig. 6). The conversion yields for $(FH_3^+)^* \rightarrow (FH_2)^*$ and $(FH_2)^* \rightarrow (FH^-)^*$ are about 0.6 and 0.8, respectively (Fig. 7), resulting in effective fluorescence yields for the cation of 0.18 ($=0.6 \times 0.8 \times 0.37$) and for the cation of 0.30 ($=0.8 \times 0.37$). This requires the deprotonation processes to be very fast, as is also suggested from the measured short fluorescence lifetime (3.1 ns compared to 3.0 ns observed upon direct excitation of the anion). The deprotonation reactions must therefore be extremely rapid, too rapid to be mediated by buffer ions, which is also evidenced from our observation that buffer concentration (0–1 M) has no effect on the fluorescence yields (results not shown). Instead the protons must be transferred to water molecules, which requires the excited cation and neutral species to be very strong acids.

In 1 M HCl novel emission is seen around 470 nm (Fig. 6) evidencing the presence of a novel emitting species. As observed previously [28], its intensity grows with increasing acidification. In 10 M HCl this emission is fully established. From its low energy onset around 450 nm, it can be ascribed to excited cation. We therefore conclude that excited cation is fluorescent at very high acidity, whereas excited neutral species has no significant fluorescence on its own under any conditions.

4.3. Fluorescein fluorescence intensity

From our characterization of the thermodynamic and spectroscopic properties of fluorescein (summarized in Table 1 and Scheme 1), it is possible to predict its fluorescence intensity in aqueous solution under a variety of conditions. Below we have summarized the factors influencing fluorescein emission in the form of an equation that allows the expected intensity to be estimated at any combination of excitation and emission wavelength, pH, ionic strength and temperature.

$$\begin{aligned} I(\lambda_{ex}, \lambda_{em}, \text{pH}, I, T) = \kappa \{ & [c_{FH_3^+}(\text{pH})\varepsilon_{FH_3^+}(\lambda_{ex})\Phi^c_{FH_3^+ \rightarrow FH_2}\Phi^c_{FH_2 \rightarrow FH^-} \\ & + c_{FH_2}(\text{pH})\varepsilon_{FH_2}(\lambda_{ex})\Phi^c_{FH_2 \rightarrow FH^-} \\ & + c_{FH^-}(\text{pH})\varepsilon_{FH^-}(\lambda_{ex})]\Phi^f_{FH^-}(\lambda_{ex})I_{FH^-}(\lambda_{em}) \\ & + c_{F^{2-}}(\text{pH})\varepsilon_{F^{2-}}(\lambda_{ex})\Phi^f_{F^{2-}}(\lambda_{ex})I_{F^{2-}}(\lambda_{em})\} \end{aligned} \quad (24)$$

The concentrations are calculated from Eqs. (8)–(10), using the appropriate apparent protolytic constants (Eq. (5)), the molar absorptivities shown in Fig. 1, the normalized emission spectra shown in Fig. 5 and the determined quantum yields. These data are available in digital form from the authors.

Acknowledgment

This work was supported by the Swedish Research Council for Engineering Sciences, the Swedish Natural Science Research Council, Magn. Bergvalls Stiftelse and by Clas Groschinkys Minnesfond.

References

[1] L.M. Smith, J.Z. Sanders, R.J. Kaiser, P. Hughes, C. Dodd, C.R. Connell, C. Heiner, S.B.H. Kent and L.E. Hood, Nature, 321 (1986) 674.
[2] Y. Cheng and N.J. Dovichi, Science, 242 (1988) 562.
[3] A.I.H. Murchie, R.M. Clegg, E. von Kitzing, D.R. Duckett, S. Diekmann and D.M.J. Lilley, Nature, 341 (1989) 763.
[4] V. Zanker, Chem. Ber., 91 (1958) 572.
[5] L. Lindqvist, Ark. Kemi, 16 (1960) 79.
[6] M. Kubista, R. Sjöback and B. Albinsson, Anal. Chem., 65 (1993) 994.
[7] W.R. Orndorff, R.C. Gibbs and C.V. Shapiro, J. Am. Chem. Soc., 50 (1928) 819.
[8] J.Q. Umberger and V.V. LaMer, J. Am. Chem. Soc., 67 (1945) 1099.
[9] M. Imamura, Bull. Chem. Soc. Jpn., 31 (1958) 962.
[10] M. Kubista, R. Sjöback, S. Eriksson and B. Albinsson, Analyst, 119 (1994) 417.
[11] P. Debye and E. Hückel, Phys. Z., 24 (1923) 185.
[12] P. Debye and E. Hückel, Phys. Z., 24 (1923) 305.
[13] P.W. Atkins, Physical Chemistry, 4th Edn., Oxford University Press, Oxford, 1990, pp. 250–252.
[14] J.E. Prue, International Encyclopedia of Physical Chemistry and Chemical Physics, Topic 15, Vol. 3, Pergamon Press, London, 1966.
[15] M. Kubista, R. Sjöback and J. Nygren, Anal. Chim. Acta, 302 (1995) 121.
[16] I. Scarmino and M. Kubista, Anal. Chem., 65 (1993) 409.
[17] M. Kubista, Chemometrics Intelligent Lab. Syst., 7 (1990) 273.
[18] G. Weber and F.W.J. Teale, Trans. Faraday Soc., 53 (1957) 646.
[19] D.M. Hercules and H. Frankel, Science, 131 (1960) 1611.
[20] P.G. Seybold, M. Gouterman and J. Callis, Photochem. Photobiol., 9 (1969) 229.
[21] R. Markuszewshi and H. Diehl, Talanta, 27 (1980) 937.
[22] V. Zanker and W. Peter, Chem. Ber., 1 (1958) 572.
[23] G. Weber and F.W.J. Teale, Trans. Faraday Soc., 54 (1958) 640.
[24] C.A. Parker, Photoluminescence of Solutions, Elsevier, Amsterdam, 1968, pp. 328–344.
[25] H. Leonardt, L. Gordon and R. Livingston, J. Phys. Chem., 75 (1971) 245.
[26] A. Weller, Progr. React. Kinet., 1 (1961) 189.
[27] M. Kasha, Discuss. Faraday Soc., 9 (1950) 14.
[28] M. Rozwadowski, Acta Phys. Polon., 20 (1961) 1005.